Proceedings World Geothermal Congress 2020+1
Reykjavik, Iceland, April - October 2021

Optimal Well Design for Stimulation of Geothermal Wells with Radial Jet Drilling

O. Leeuwenburgh[1,2], E. Peters[1], D. Troost[2], H. Cremer[1]

[1]TNO, Princetonlaan 6, Utrecht; [2]Delft University of Technology, Delft

Corresponding author: lies.peters@tno.nl

Keywords: Radial jet drilling, well design, geothermal energy, optimization, uncertainty quantification

ABSTRACT

Geothermal wells can be stimulated to increase productivity or injectivity by drilling multiple, small-diameter laterals using a technique called Radial Jet Drilling (RJD). One would like to design the placement of these laterals such that an optimal connectivity with the reservoir is achieved. Since there is large flexibility in the design in terms of number of laterals, the along-well kick off depth, and the orientation and length of laterals, as well as complex interaction between the dynamic effects of changes in the design, determining the optimal design may be fairly challenging. This complexity is further increased if the reservoir is heterogeneous or if the distribution of rock properties and the trajectories of laterals are uncertain. Here we will investigate the sensitivity of the geothermal system performance to the design parameters for an example case involving a pair of geothermal wells positioned in a reservoir with properties typical for the Dutch setting. We will investigate the sensitivity directly by simulating different scenarios for the design parameters, and we subsequently explore the potential to use numerical optimization techniques to find optimal values for these parameters. Both (local) gradient-based and (global) evolution strategies are considered and we comment on advantages and disadvantages of both in the context of the design of geothermal wells. We find that both approaches are able to deliver improved designs in different settings, but that stochastic gradient methods may be best suited for design optimization under geological uncertainty.

1. INTRODUCTION

Geothermal wells can be stimulated to increase productivity or injectivity by drilling multiple, small-diameter laterals using a technique called Radial Jet Drilling (RJD). In this technique, multiple laterals with lengths up to 100 m and a diameter of 25 to 50 mm are created using hydraulic jetting (see e.g. Kamel, 2017, Yan et al, 2018). A typical design is, for example, to jet 8 to 16 laterals in a single well in groups of 4 per kickoff point with a spacing between laterals at each kickoff point of 90° (Figure 1). The kickoff points can in principle be positioned anywhere along the length of the backbone. Their positioning can therefore be chosen to achieve an optimal productivity or injectivity for an individual well, or for the performance of a geothermal doublet as a whole. In the presence of geological heterogeneity, the effect of alternative placings may be difficult to predict without the use of a numerical simulation model. If such a model is available, alternative placings can be tested and compared. In fact, the entire design of each well can be evaluated and optimized by means of numerical optimization methods. The use of model-based optimization for field and well design has been the subject of numerous studies in the petroleum industry. Recent developments in that field include the optimization of the trajectories of a fixed set of wells that are to be drilled from a single offshore platform (see, e.g. Barros et al., 2018). Examples of applications to geothermal field development include the studies of Ansari et al. (2014), Chen et al. (2014), Helgason (2017), and Kong et al. (2017) which are generally limited to the placement of vertical wells. In contrast, applications of numerical optimization methods to multi-lateral well-design has been very limited so far and has, to the best of our knowledge, been limited to oil well design only (Abukhamsin, 2009).

Here we are interested in investigating the possibility of determining an optimal design for the RJD stimulation of a geothermal well or doublet, where the design is defined by the placement along given backbones of an a priori unknown number of radials that are associated with an a priori unknown number of kickoff points. The optimality of the design will typically be determined by the difference between additional costs to drill radials and the extra monetary revenues that are obtained as a result of the improved performance of the geothermal system.

The design parameters of the sketched optimization problem include both integers (number of laterals per kick-off, number of kick-offs) and real numbers (spacing between kick-offs and between laterals within a single kick off, lateral orientation). The presence of integer design parameters potentially makes the general design problem unsuited for direct solution with gradient-based methods. Here we will therefore consider the Covariance Matrix Adaptation Evolutionary Strategy (CMA-ES) method from the family of population-based optimization methods (Hansen, 2016). Design problems that do not include integer design parameters could be addressed using gradient-based optimization methods. In some cases it may be possible to re-parameterize problems in terms of continuous parameters, resulting in a problem that can be solved using gradients. The main benefit of using a gradient-based method is the high computational efficiency. Recent developments in stochastic gradient methods have made it possible to extent this efficiency also to cases with model (geological) uncertainty (Chen, 2008; Fonseca et al., 2014).

Since the laterals are not steered but rely on the stiffness of the jetting hose to keep a straight path, the actual achieved path of the laterals is also uncertain (Reinsch et al., 2018). This uncertainty has considerable impact on the expected enhancement of the flow (Nair et al., 2017; Peters et al., 2019b) and should ideally be accounted for when the optimality of a particular design is evaluated. We would ideally like to identify designs that are somewhat robust to deviations from the planned trajectories of the laterals. While an experimental implementation is available of an uncertainty-handling version of CMA-ES (Hansen et al., 2009; Troost, 2019), here we will present results from a sensitivity study into the effect of uncertainty in the laterals' paths only.

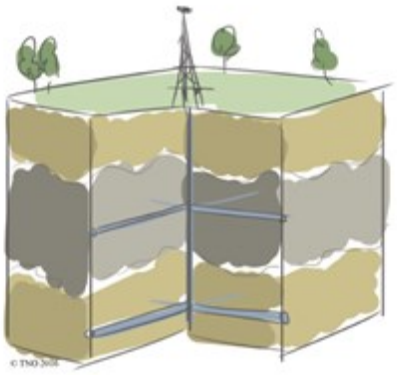

Figure 1: Conceptual illustration of a single vertical backbone and two kick-offs with four radials each spaced at 90°.

In the remainder of this paper we will define the objective function that we wish to maximize, describe the design parameters, introduce the simulation and optimization methodology, and show results of the application of the optimization workflow to a geothermal doublet.

2. METHODS

2.1 Radial jetted well simulation

In order to evaluate different RJD designs, we need to be able to simulate the impact of a particular design on the flow dynamics. The inflow or outflow of each radial into the reservoir q_i is determined by the pressure difference and connectivity WI_i between the in the radial $p_{w,i}$ and the grid block $p_{b,i}$ in which the radial is located:

$$q_i = \frac{WI_i}{\mu}\left(p_{b,i} - p_{w,i}\right) \tag{1}$$

where μ is the viscosity of fluid. The connectivity or Well Index WI_i can be computed individually for all intersections of the radial trajectory with the intersecting grid cells using the projection method or three-part Peaceman formula (Peters et al., 2018; Peters et al., 2019a). In this method the intersection of a well with a grid cell is projected on a local coordinate system. For each of the three projected parts, the WI is calculated and the results are subsequently combined into a single WI_i. This calculation has been incorporated in a stand-alone tool based on the open source code FieldOpt (NTNU, 2018) which has been extended further to allow for well index calculation for multilateral wells. The accuracy of this calculation is very important for sensitivity calculation and for optimization. If the accuracy is insufficient, numerical errors may be larger than the differences resulting from different parameter sets. The accuracy of the projection approach was tested by comparison with the results of other simulators (Peters et al., 2018). In addition, Troost (2019) evaluated the accuracy of the simulation, in particular the effect of changing the azimuth of radials. Both studies concluded that for a sufficiently fine grid (< 10 m), the error is in the order of a few percent, which is probably sufficiently small for the optimization. The calculated well indices are input for a reservoir flow simulation. All flow simulations presented here were performed with the open-source simulator Flow that has been developed as part of the Open Porous Media (OPM) initiative (opm-project.org).

2.2 Definition of the optimization problem

In order to evaluate and compare alternative designs a performance measure needs to be determined. Here we will adopt an economic performance measure that includes the costs of drilling additional radials and the revenues associated with increased heat recovery. We define Net Present Value (NPV) of the project as

$$NPV = \sum_{t=0}^{n} \frac{P(t)}{(1+r)^t} \tag{2}$$

Where $P(t)$ is the total of costs and revenues incurred at time t. The discount rate r is taken as zero in this application. The costs for jetting radials depends on a number of factors, including rig rate and mobilization cost, duration of the job and preparation cost. The last item can also include additional logs that need to be run in preparation or extended planning/simulation of the radial design. The total cost and the relative contributions of the different factors depend very much on the specifics of the job. For the optimization, the most important is that the incremental cost and benefits of adding radials are properly accounted for. To achieve this, we assume that the main cost component can be represented by a linear function of time; the more radials need to be jetted, the more time it takes and the more expensive it becomes. The upfront costs are thus not taken into account explicitly. If only a single well is stimulated this means that our cost will be lower than the actual one. Assuming a daily cost of €60,000 and a drilling efficiency of 2.2 radials per day, the capital expense amounts to €27,000 per radial. The costs of drilling the backbone and well operation costs do not need to be considered because only the incremental cost and benefit of the radials are included in the analysis.

The revenues of the radials are proportional to the incremental amount of heat Q produced by the radials with $Q = m \cdot c_p \cdot \Delta T$ where m is the incremental mass of produced water by the laterals, c_p is the heat capacity of water, and ΔT is the difference in temperature between produced water and re-injected water. For this application it is assumed that the temperature difference is constant over

time at 60 °C (80°C production temperature and 20°C injection temperature). The wells are operated at a fixed pressure which means that the pump fuel usage depends on the flow rate only. The produced heat is translated to a monetary benefit via the price of heat of 0.02 euro/kWh (Lensink et al., 2018). Because it is not clear what the life time of the radials will be (Peters et al., 2019b), we assume that the radials produce at the same rate for three years, i.e. the incremental mass produced by the radials for three years is used for the calculation of Q. It should be noted that both cost and benefit contributions to the NPV are simplified and that the calculated NPV for the two case studies are thus not fully representative of a real NPV for a radial jetting case.

We will now discuss the design parameters that will act as the decision variables in the optimization problem. A single, straight lateral can be characterized by the following set of parameters: kickoff depth, length, diameter, azimuth and inclination. To simplify the optimization, at this stage the laterals are all assumed to be 100 m long and have a fixed diameter of 0.05 m. Also inclination is not used here as a design parameter and is fixed at an angle of 90° with the backbone. The laterals are grouped in kick-offs and the following design parameters are used per kickoff: position (depth) between top and bottom of the reservoir (normalized from 0 to 1) and number of laterals.

The azimuth of each lateral can be controlled via the orientation of the deflector shoe. For a vertical well in a laterally homogeneous reservoir, this may not be very relevant, but for deviated wells this can be important since the azimuth will affect the absolute inclination of the lateral with respect to the vertical and therefore result in accessing different layers, or possibly even in extension of the lateral into the overburden or underburden. Therefore azimuth is used as a design parameter which should be optimized. We introduce an additional parameter that we refer to as the 'window', which controls the azimuth angle over which the laterals are distributed. The standard placement is to use a window of 360 degrees, resulting in 90 degrees angles between 4 laterals. These 4 laterals could alternatively be distributed over a half circle of 180 degrees, thus directing all laterals towards one side. The concept is illustrated in Figure 2.

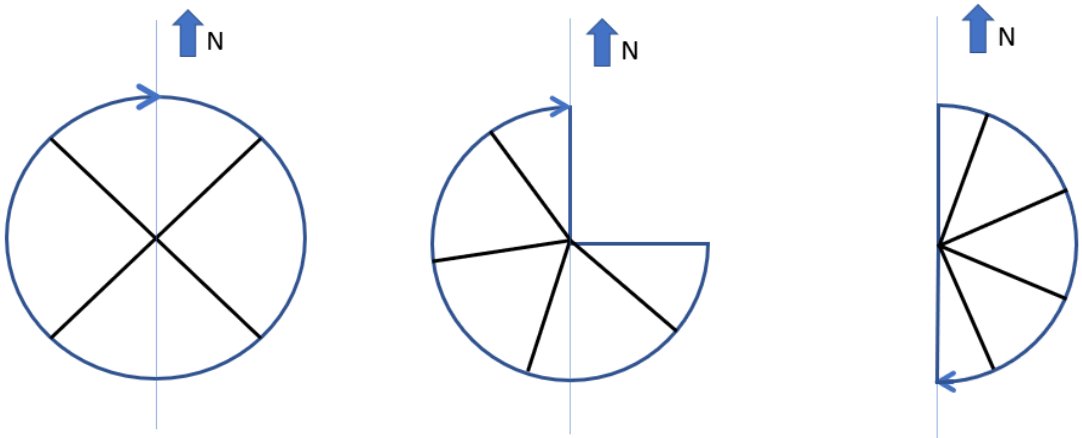

(a) (b) (c)

Figure 2: Illustration of the window design parameter: distribution of 4 radials over a window of (a) 360° , (b) 270° and (c) 180°.

The final design parameter is the number of laterals at 5 each individual kickoff. This parameter can only take integer values and therefore makes the optimization problem unsuited for (exact) gradient-based strategies. It may be possible to use a parameterization of this design aspect, for example in terms of angles between laterals, turning the problem into a continuous problem. We have investigated the use of a simple continuous scalar parameter that we round to the nearest integer value.

2.3 Solution Approach

2.3.1 Covariance Matrix Adaptation Evolution Strategy (CMA-ES)

CMA-ES (Hansen, 2011; 2016) is a population-based optimization strategy that evaluates a set of perturbed parameters sampled from an initial distribution, ranks them according to the performance measure, updates the distribution, and samples a new set of parameters from the updated distribution. This process is repeated until convergence when the performance of the distribution mean does not improve anymore. The updates of the distribution involve separate updates of the mean m and of the covariance matrix C. The update equations are

$$m^{k+1} = \sum_{i=1}^{\mu} w_i \, x_{i:\lambda}^{k+1} \tag{3}$$

where m^{k+1} is the mean parameter vector at iteration $k + 1$, based on weighting by weights w_i of the best μ members of the population that consists in total of λ members x_i,

$$p^{k+1} = (1 - c_c)p^k + \sqrt{c_c(2 - c_c)\mu_{eff}}\,\frac{m^{k+1} - m^k}{\sigma^k} \tag{4}$$

where p^k is the so-called evolution path vector, and all other variables are tuning parameters.

The update equation for the covariance matrix is

$$C^{k+1} = (1 - c_1)C^k + c_2 p^{k+1} p^{k+1^T} + c_3 \sum_{i=1}^{\mu} w_i \, y_{i:\lambda}^{k+1} y_{i:\lambda}^{k+1^T} \quad (5)$$

where y_i^{k+1} is a normalized member of the population at iteration k. The second and third terms in Eq. [5] are referred to as the rank-one and rank-μ updates respectively. Once a new mean and covariance matrix are determined, new samples can be generated from the resulting Gaussian distribution as characterized by the new mean and covariance matrix. Default values exist for all tuning parameters of the CMA-ES algorithm. We have adopted the values proposed by Hansen (2016).

We assume here that all radials are drilled as planned, which may not be the case in reality. In a related study (Troost, 2019) we applied a variation of the generic CMA-ES algorithm modifications that can be used to handle uncertainty (Hansen et al., 2009) based on re-evaluation of selected population members after perturbation in accordance with the prescribed uncertainty. For more details the reader can consult the referenced publications.

2.3.2 Stochastic gradients (StoSAG)

The idea behind gradient-based optimization strategies is to update a single strategy using the derivative of the objective function with respect to the parameter values (the gradient). If the derivatives are not available they can be estimated numerically. A simple but generally computationally unattractive approach is to perturb each parameter individually and perform simulations for each perturbed parameter vector. More efficient approaches include the so-called stochastic gradient approximation methods such as SPSA (Spall, 1995) and ensemble gradients, in particular the Stochastic Simplex Approximate Gradient (StoSAG) (Chen , 2008; Fonseca et al., 2014; Fonseca et al., 2017). An advantage of numerical gradient approximation methods relative to exact gradients that is that strict continuity or smoothness is not required. Furthermore, the StoSAG method provides a computationally attractive extension of the idea behind ensemble gradients to the setting with uncertain models. A single design solution is optimized through an iterative update process. A typical line search strategy is defined as follows,

$$\boldsymbol{m}^{k+1} = \boldsymbol{m}^k + \sigma \boldsymbol{g}^k \quad (6)$$

The stepsize σ is normally kept constant throughout the optimization although it could be adapted. The gradient is estimated from a finite set function evaluations for perturbed ensemble members with index i = 1, …, N_e

$$\boldsymbol{x}^i \sim \boldsymbol{m}^k + \mathcal{N}(0, C_{\boldsymbol{m}}) \quad (7)$$

The gradient is obtained as

$$\boldsymbol{g}^k = \boldsymbol{X}^{\dagger} J \quad (8)$$

where the right hand side consists of the generalized pseudo inverse of the matrix that has the perturbation vectors as its rows, and the column vector J with objective function deviations with respect to the objective function value for the current control. These are the equations for the deterministic optimization case. In the setting with uncertainty the evaluation of objective function values becomes a function of both the control and the model realization and the gradient should be interpreted as the gradient for the expected objective function value.

3. EXPERIMENTS AND RESULTS

3.1 Model description

We consider a typical geothermal development, namely a so-called doublet, consisting of 1 injector and 1 producing well. Complexity arises from the fact that both wells are deviated and from a permeability gradient resulting in reduced injectivity at the location of the injection well. The deviated nature of the trajectory of the injection well means that permeability is lower near the toe of the well (near the bottom of the reservoir) than at the entry point, which is located closer, laterally speaking to the producer. The reservoir is relatively thin and the entire well section inside the reservoir is available for stimulation. This could potentially mean that jetted radials, which we will assume to have a length of 100 m, may leave the reservoir, depending on the kickoff depth and orientation, significantly decreasing their effectiveness, and possibly violating design constraints. This could be mitigated in different ways, e.g. by placing them in the middle of the reservoir or by placing them high and orient them downwards. However, placing all laterals close together in the middle of the reservoir will reduce their efficiency due to interference. Placing the laterals at the top or bottom, is a less robust strategy, because the un-steered radials could leave the reservoir. To complicate matters further, permeability is higher at the top of the well than at the bottom. As a first step, a number of scenarios is calculated manually to see what the difference is between the scenarios. Next the model is optimized using numerical optimization tools.

The reservoir model is 100 m thick and 1.5 by 3 km wide (Figure 3). Both wells are deviated with an angle of 40° and the wells have an average distance of around 1500 m at reservoir depth. An overview of the input settings for the reservoir is given in Table 4 4 and a top view of the model showing the permeability in Figure 3.

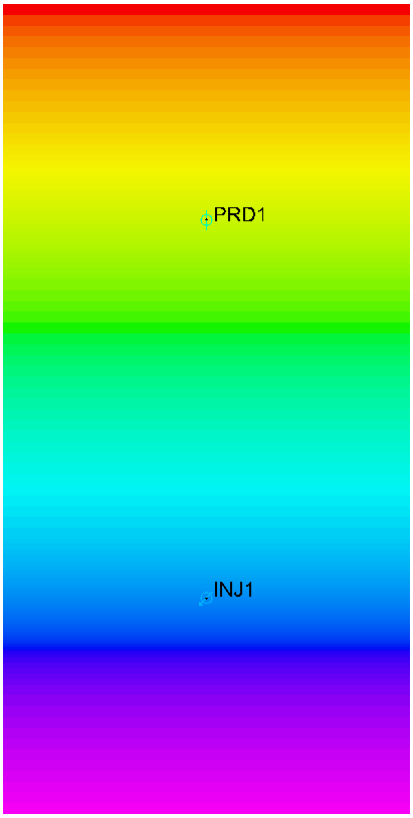

Figure 3: Top view of the reservoir with permeability gradient indicated in color and the position of the injector (INJ1) and producer (PRD1) well (red is high).

Table 1. Characteristics of the model test case

Grid dimensions	89 x 188 x 40
Cell size	40 m, 5 m around wells, 2.5 m thick
Horizontal permeability	20 – 200 mD
Porosity	0.1
Vertical permeability	Hor. Permeability/5
Fluid salinity	30 g/l
Reservoir pressure	190 bar at 1900 m
Well inclination	40 deg
Well azimuth	180 deg (injector), 0 deg (producer)

The wells are run on pressure constraint. The pressure difference between the injector and producer is 40 bar (210 bar for the injector and 170 bar for the producer). The steady state rate of the doublet without stimulation is only 1400 sm^3/d (58 sm^3/hr). This low rate is the result of the low permeability of the reservoir, which ranges from 20 to 200 mD. Thermal effects have not been included in the analysis. This means that overall the injectivity of the injector is overestimated compared to the productivity, due to the effect of the higher viscosity of cold water. However, this does not affect the optimization results, because it is the same for all simulations. Also because the doublet is simulated in a closed system, the rates of the injector and producer quickly become the same.

We consider a base design with 2 kickoff points and 4 jetted radials drilled from each kickoff point. Breakthrough of cold water does not play a role for the optimization: well distance is large and the rate is low and thus breakthrough does not occur within 30 years. In order to evaluate the effect of drilling radials we do not need to simulate this entire period, but can extrapolate the results from a short simulation until steady-state is reached and extrapolate over the life cycle period.

3.2 Sensitivity experiments

Before the optimization, it is investigated manually what the results are for different scenarios. For this reservoir, the main control on the increase in flow performance achieved by the radial stimulation is whether the radials stay in the reservoir or not. Since the reservoir is only 100 m thick and the radials are assumed to be straight and 100 m long, the radials can leave the reservoir easily. Three different scenarios were investigated, which all have two kick-offs and 4 radials per kick-off:

- Standard case: the kick-offs are placed at one quarter and at three quarters of the depth of the reservoir (Figure 4)
- Mid case: the kick-offs are placed close to the middle of the reservoir, which is robust for deviations in path of the radials.
- Optimal case: the kick-offs are placed in such a way in the reservoir, that they cover the thickness of reservoir as good as possible. One kick-off is placed near the top of the reservoir with radials pointing down and one kick-off is placed near bottom of the reservoir pointing upwards (Figure 5).

For the first two cases, the angle between the radials is 90°. For the third case, the angle between the radials is 45° (except for the first and last radial). Only in the Optimal case are the radials entirely contained in the reservoir. The cost for all cases is identical, namely 8 x €27 k€ = 218 k€ (see Section 2.2 for a discussion of the cost). The benefits in case of perfect radials (i.e. exactly as specified in the design) is listed in Table2. The benefit is calculated as specified in Section 2.2, i.e. with a temperature difference of 60° and with the increase in rate compared to the unstimulated rate over a period of 3 years. For the Optimal case, which shows the highest benefits, the rate increases from 1400 sm3/d to 2168 sm3/d which is an increase of 55%. The benefit ranges from 1028 k€ to 1181 k€.

Table 2 Overview of scenarios for the Doublet model with flow rate and estimated benefit.

Case Name	Relative kick-off depths (-)	Azimuth first radial per kick-off	Steady state flow rate of the doublet (sm^3/d)	Benefit (k€)
Standard	**0.25, 0.75**	**45°, 45°**	**2065**	**1028**
Mid	**0.45, 0.55**	**0°, 45°**	**2087**	**1061**
Optimal	**0.1, 0.9**	**-67.5°**	**2168**	**1181**

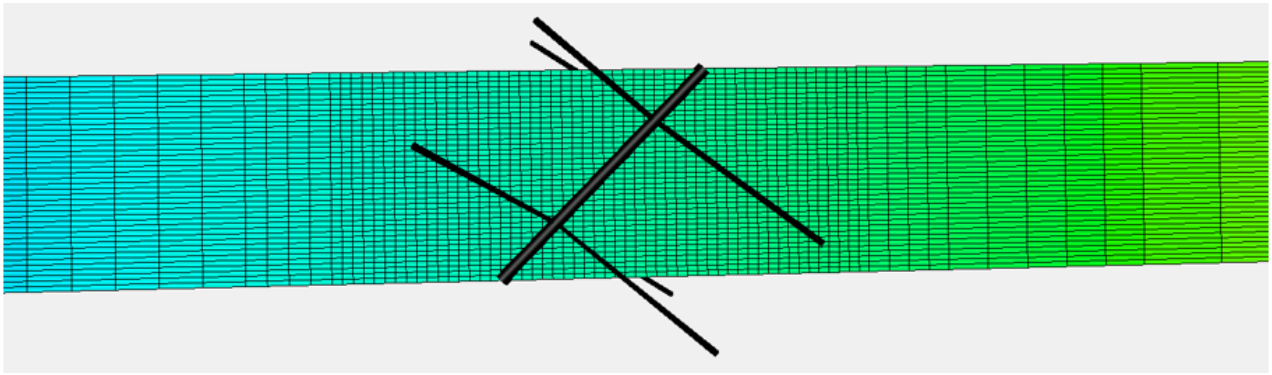

Figure 4: Side view of the injector wells with radials as in the Standard case (See Table 2): 2 kick-offs at 25% and 75% of the depth with 4 radials each.

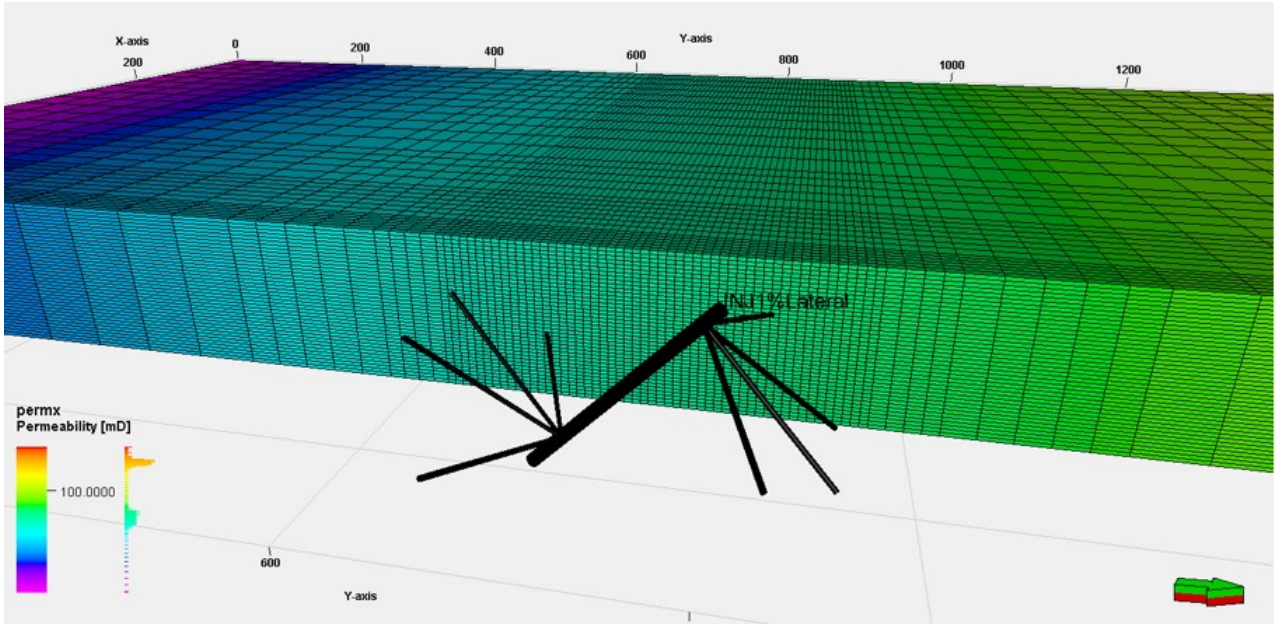

Figure 5: Illustration of the injector well with radials in the Optimal case (see Table 2): 2 kick-offs at 10% and 90% of the depth with 4 radials each.

The steady state rate for the Standard case becomes a bit higher if the radials at the second kick-off are rotated 45° compared to the first kick-off, namely 2075 sm^3/d.

The estimates in Table 2 do not take into account the uncertainty in the radial path. This can however have a significant impact on the results. To account for uncertainty in the radial path, the simulations were repeated with the different radial paths. 30 Realizations of the radial paths were made and the resulting flow simulated. The realizations were created by sampling from uniform uncertainty ranges for kick-off depth, length, azimuth inclination and diameter of the laterals. Sampling was done according to a Latin Hypercube scheme. The uncertainty ranges are presented in Table 3. Absolute ranges mean that the values used in the simulation are sampled from that range. Relative ranges means that the values sampled from the range are added to the base value, e.g. for the kick-off depth. The range of the radial diameter is quite large, because this includes potential effects of skin and viscous pressure drop due to flow in the lateral. Nair et al (2017) showed that the impact of radial diameter is relatively small.

Viscous pressure drop was shown to be important because of the very irregular and rough inner diameter of a lateral compared to normal tubing (Peters et al., 2019) and. Inclination is defined as an absolute range assuming a horizontal base position of the radial.

The representation of the uncertainty in the lateral path is simplified here, since the laterals are always assumed to be straight and uniform along their entire length. Curvature as observed in Reinsch et al. (2018) is not accounted for.

Table 3. Uncertainty quantification for the radials

	Type of uncertainty	**Minimum value of the range**	**Maximum value of the range**
Length (m)	Absolute	10	100
Diameter (m)	Absolute	0.001	0.1
Inclination (°)	Absolute	20*	160*
Azimuth (°)	Relative	-90	90
Kick-off point (m)	Relative	-2	2

* 90° is horizontal.

The results when taking into account uncertainty are presented in Table 4. The average steady state flow rate of the doublet over the 30 realizations is given and the average benefit. Also the minimum and maximum benefit realized in the 30 realizations are presented to identify potential low and potential for upside. The average flow rate and benefit are much lower and much closer together than for the perfect laterals. The optimal case has the lowest benefit, because the radials run a high risk of going out of the reservoir. The kick-off points were at 10% and at 90 % of the depth. The mid and standard case show similar results. The end is clearly lowest for the optimal case. In fact, since the cost is estimated at 218 k€ (not taking into account the up-front costs), the benefits are only just higher than the cost for this case.

In conclusion, we see that the case which is optimal in case of perfect radials has the least robust results. When taking into account the uncertainty, this case has the lowest benefits and the highest risk of very low results.

Table 4. Estimates of the flow rate and benefit including uncertainty (for range see Table 3) for three scenarios for the doublet (average of 30 realizations).

	Average flow rate (sm^3/d)	**Average benefit (for 3 years in k€)**	**minimum benefit from 30 realizations (k€)**	**Maximum benefit from 30 realizations (k€)**
Standard	1865	729	569	913
Mid	1867	733	620	889
Optimal	1842	695	300	907

3.3 Optimization experiments

3.3.1 Deterministic optimization of design parameter subsets

Here we consider a number of test cases based on optimization of different subsets of design parameters. These experiments are chosen to test different aspects of the parameterization before embarking on more complex and complete joint optimization of the full set of design parameters, including geological uncertainty.

This first experiment has only 2 design parameters, namely the depths of the 2 kickoff points. The depths are represented in terms of fractions of the full vertical depth interval. Since this represents continuous controls, an optimization approach based on ensemble gradients should work. We use small ensemble of 5 samples only, which results in a computational cost that approximately equal to that associated with simple finite two-sided difference gradients. It is assumed that 4 laterals are drilled by radial jetting, with the first lateral oriented north, and the others distributed evenly (i.e. with 90 degree intervals) over the 360 degree window. The experiment serves as a check on the implementation and is simple enough to be able to predict the main features of an optimal design. Since there is a lateral trend in the permeability of the rock matrix, and the injector follows a deviated path, we expect the kickoffs to be placed in the depth interval with higher permeability. Initial kickoff points were placed at fractions of 0.25 and 0.75 of the full depth interval (as measured from the top) while final values after optimization with ensemble gradients were 0.17 and 0.53. So both kickoff points were moved upward somewhat, consistent with our expectation. The two points are kept somewhat separate, presumably to avoid interference. Also, the orientation of the 4 radial laterals is kept fixed at 90 degree intervals. One of the radials drilled in each kickoff point will therefore extend outside of the reservoir zone. The optimization is likely to penalize further upward movement since this would reduce the effectiveness of one of the radials. The improvement in NPV over 10 iterations is illustrated in Figure 6(a).

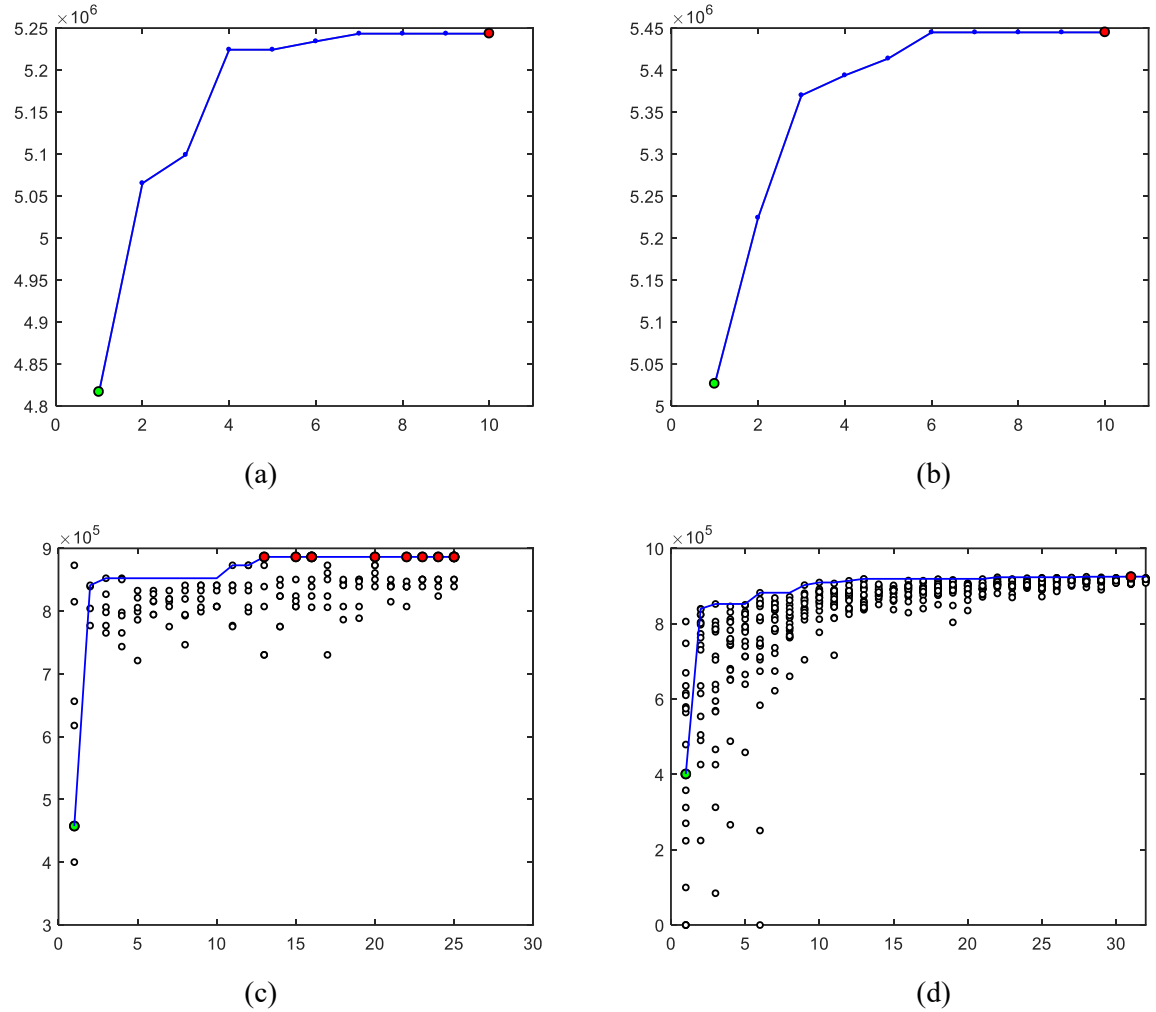

Figure 6: Evolution of NPV as a function of iteration number for 4 deterministic experiments. (a) Optimization of the kickoff point depths using ensemble gradients. (b) Optimization of the orientation of a fixed number of radials in two kickoff points using ensemble gradients. (c) Optimization of the number of radials in two kickoff points assuming an even distribution (orientation) using CMA-ES. (d) Joint optimization of the number and orientation of radials in two kickoff points using CMA-ES.

Figure 6(b) shows the NPV evolution for a deterministic optimization of the orientation of the radials (azimuth and window) for a design with 4 radials and two fixed kickoff points. A clear continuous improvement in NPV is observed over 10 iterations, similar to the optimization of kickoff depth only. In absolute terms the improvement is limited for these two cases. A third design parameter of interest is the number of radials drilled in each kickoff point. We use this case to test the CMA-ES algorithm. While we use a continuous parameterization of the number of radials, the objective function will show non-continuous behavior which may make this case challenging for a gradient-based approach. The optimization is started with initial values of 1 (1 radial in each kickoff point only), explaining the relatively low initial NPV value. When additional radials are added, they are placed at equal angle intervals dividing up the complete 360 degree window and the initial strategy is to only drill one radial at each kickoff point. In the mean solution obtained after 17 iterations, 9 radials are drilled at each kickoff point. The evolution of all 6 samples, as well as the mean, is shown 20 Figure 6(c). It can be seen that a systematic improvement is obtained, and that the population spread tends to decrease when the optimum is approached. Finally, Figure 6(d) shows results from an optimization of both the number and the orientation of radials using CMA-ES. This experiment was not continued up to convergence. The initial iterations show fairly consistent improvement, however, suggesting that also joint optimization problems (with multiple control types) can be solved using CMA-ES.

3.3.2 Deterministic optimization of kickoff depths and number and orientation of laterals

The purpose of this experiment is to optimize the full set of design parameters. Since this is a deterministic optimization problem that includes a discrete design parameter (number of laterals for each kickoff) that produces a non-continuous objective function, we first apply the CMA-ES algorithm. The number of kickoffs was set to 2 and the population size was fixed to 20. The iteration process was continued for 24 iterations and stopped before convergence for practical reasons. Results are shown in Fig. 7 and Fig. 8. The NPV values in Fig. 7 show a consistent improvement over the first few iterations while the large spread may be reflecting the global search strategy resulting from the use of large perturbations. The spread is reduced during later iterations, when the algorithm takes on a more local search character that enables the identification of the optimum at iteration 15. It is possible that further improvements could have been obtained by continuing the optimization beyond 24 iterations. The maximum NPV value is

close to that obtained for optimization of the number of laterals only, which appears to be the dominating factor in the design. Figure 8(a) shows that the number of radials is changed from 4 to 10 in both kickoff points. Only the azimuth for the second (lower) kickoff has a comparable relative change in the value of the parameter. However, the window size is maximized at 360 degrees, which means that the azimuth is not that relevant when 10 radials are drilled. The depths of both kickoff points are reduced, consistent with the result of the kickoff depth-only experiment.

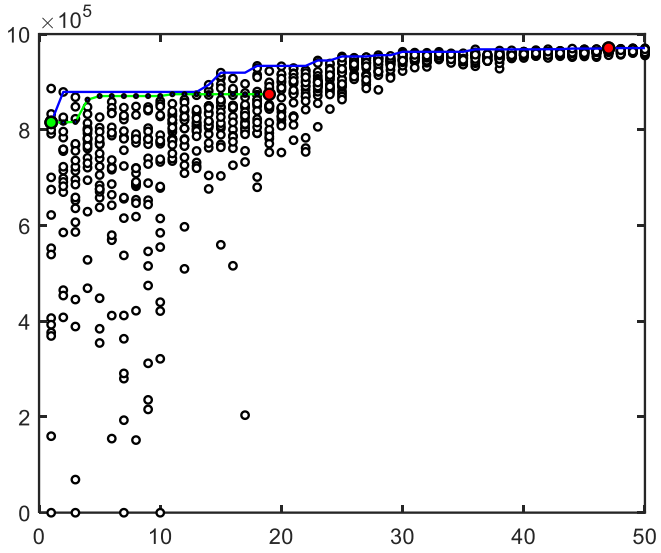

Figure 7: Evolution of a 20-member population over 24 iterations of the CMA-ES algorithm (black circles). Controls include the depths of 2 kickoff points, and the number and orientation (through the azimuth and window) of laterals drilled at these kickoff points. The initial strategy is indicated by the green dot, the overall best by the red dot, and the blue line indicates the current best. The NPV evolution for the same problem obtained using StoSAG is indicated by the magenta line (the optimization had not yet converged after 17 iterations).

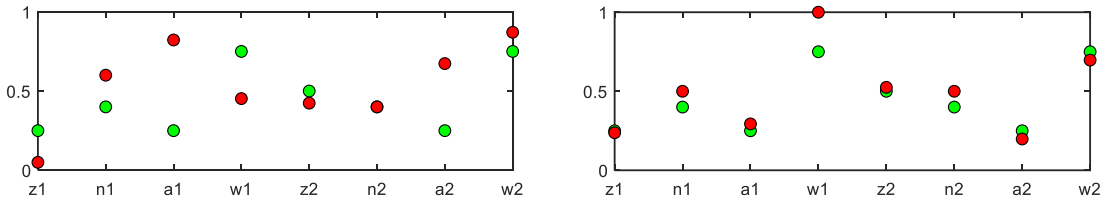

(a) (b)

Figure 8: Initial (green) and optimized (red) values of the design parameters for kickoffs 1 and 2: depth (z), number of laterals (n), azimuth (a) and window (w), as estimated using (a) CMA-ES, (b) StoSAG.

The optimization problem including the full set of parameters was also addressed using the StoSAG algorithm. After some initial iterations without much improvement a fast increase in NPV was obtained (Figure 7). After 17 iterations the process had not yet converged, but already a higher NPV was obtained than with CMA-ES. An ensemble size of 20 members was used for gradient estimation, identical to the population size used with CMA-ES. An additional 1 to 3 simulations were performed per iteration within the line search scheme. The estimated parameter values are very similar to those obtained with CMA-ES as illustrated in Figure 8(b). The main difference is in the sign of the change in the azimuth which defines the orientation of the first radial. This primarily affects the first kickoff, which has a window smaller than 1 (corresponding to 360 degrees). We may conclude that StoSAG can be used to also solve non-continuous problems (the number of radials is included as a design parameter), and is likely to be more computationally efficient than CMA-ES more optimization problems with large parameter sets.

3.3.3 Robust optimization of kickoff depths and orientation of laterals

Here we wish to demonstrate the possibility to optimize lateral well design in the presence of geological uncertainty. We generated 20 possible geological realizations of the geothermal reservoir by adding perturbations to the reference permeability and consider the robust optimization problem of maximizing the expected value of the objective function value. The expected value is computed simply as the average over all 20 realizations. Since there is no efficient extension available as yet of the CMA-ES algorithm for such cases, and since we consider only continuous design parameters, this problem was addressed using the StoSAG method based on approximate ensemble gradients.

Figure 9 shows the evolution of the 20 individual ensemble member values as well as the expected value over the iteration process for a robust optimization of kickoff depth and orientation of a fixed number of laterals under geological uncertainty. The spread of the gray lines indicates the impact of the geological uncertainty on the economics at each subsequent iteration, corresponding to a new proposed design, which is quite large. Despite this uncertainty, the persistent increase in the objective function value indicates that the method is able to find designs that maximize the economics. The improvement is slow however, due to the varying impact that the uncertainty appears to have on the performance of each design for different geological realizations. This variable impact is reflected by the crossing of lines, meaning that a change in design may work better for one realization than for another one. This variability results in very small step sizes, corresponding to correspondingly small incremental changes to the design. We note, however, that only 20 simulations are required to estimate a new direction for adjustment of the design, whereas for a method like CMA-ES this number needs to be multiplied by the population size.

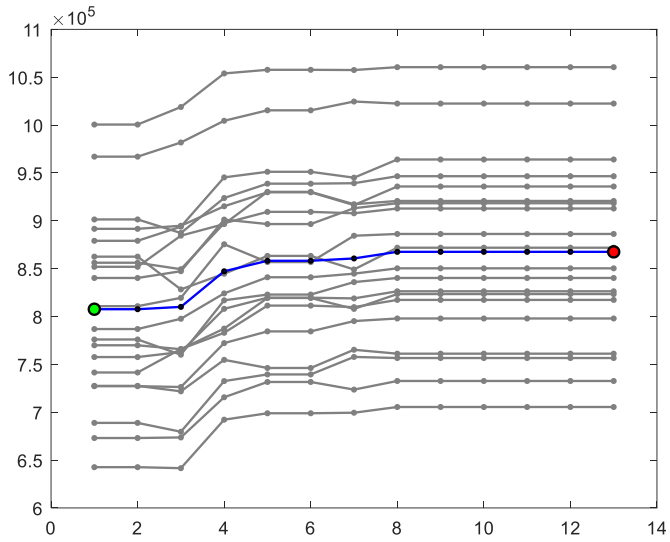

Figure 9: Evolution of a 20-member ensemble over 13 iterations of the StoSAG algorithm. Controls include the depths of 2 kick off points and the number and orientation (through the azimuth and window) of laterals drilled at these kickoff points. The initial strategy is indicated by the green dot, the overall best by the red dot, and the blue line shows the evolution of the expected value.

4. CONCLUSIONS

We have explored the impact of different designs for geothermal well stimulation by Radial Jet Drilling. This could potentially be an attractive way to enable the production of heat from relatively poor quality reservoirs and an alternative to conventional hydraulic fracking. We consider designs for stimulation of the injector well of a geothermal doublet consisting of an injector and producer well with deviated well trajectories. The designs are characterized by a set of design parameters that include the depths of kickoff points, the number of radials in each kickoff, and the orientation of the radials.

A sensitivity study into the impact of alternative designs show that the effect of these parameters on the flow dynamics, and consequently on the project economics, is significant. This sensitivity can be related to the non-homogeneous character of the reservoir and the deviated nature of the backbones, resulting in a injectivity trend along the well backbone as well as a risk that radials extend outside of the reservoir, but also due to the possible interference between neighboring, closely placed radials. The combination of these complexities and the geological uncertainty that will be present in real applications makes it practically impossible to identify an optimal design without significant computational expense.

We therefore investigated the possibility of using numerical optimization techniques to find optimal designs at relatively low computational cost. Since the design problem with integer parameters constitutes a mixed-integer optimization problem we consider both a global evolution strategy type approach and a stochastic gradient approach.

Initial experiments involving only subsets of parameters show that the optimization approach should be feasible, as evidenced by significant improvements in project NPV over relatively few iterations. A solution of the full deterministic design problem was obtained using the CMA-ES algorithm, which suggested that the number of radials is the most important design parameter for this problem. Since CMA-ES does not show attractive scaling in terms of computational cost when geological uncertainty is considered, we applied an ensemble gradient technique (SToSAG) to find an optimal design in that setting. We could demonstrate consistent improvement of the expected project economics despite a very large sensitivity of the performance to the unknown permeability distribution. This large sensitivity may be an artifact of the increased resolution that we created in the numerical grid around the wells. A lower small-scale heterogeneity will results in a smoother response and more well-behaved optimization problem.

Further steps could include testing of parameterizations of the number of kickoffs and radials for use in stochastic gradient approaches, as well as the addition of parameters characterizing the trajectory of the backbone of both injector and producer wells.

ACKNOWLEDGEMENTS

The SURE project has received funding from the European Union's Horizon 2020 research and innovation programme under grant agreement No 654662. The content of this presentation reflects only the authors' view. The Innovation and Networks Executive Agency (INEA) is not responsible for any use that may be made of the information it contains. The authors acknowledge valuable input and discussions with Thomas Reinsch (GFZ) and other partners in the SURE project consortium. The help of NTNU with implementation of the WI calculation is gratefully acknowledged. The use of open source codes Field-Opt by NTNU and OPM-flow (https://opm-project.org/) is gratefully acknowledged.

REFERENCES

Abukhamsin, A. Y., Optimization of well design and location in a real field, MSc Thesis, Stanford University, 2009.

Ansari, E., Hughes, R. and White, C.D., 2014: Well placement optimisation for maximum energy recovery from hot saline aquifers. *Proc.* 39th Workshop on Geothermal Reservoir Engineering, Stanford University, Stanford, USA, February 24-26.

Barros, E., Chitu, A., and Leeuwenburgh, O.: Ensemble-based optimization of well trajectory design in the Olympus Field, EAGE/TNO Workshop on OLYMPUS Field Development Optimization, 7 September 2018, Barcelona, doi:10.3997/2214-4609.201802294.

Chen, M., Tompson, A.F., Mellors, R.J. and Abdalla, O., 2014: An efficient optimisation of well placement and control for a geothermal prospect under geological uncertainty. *Applied Energy* 137 352-363. https://doi.org/10.1016/j.apenergy.2014.10.036

Chen,Y., 2008: Ensemble-based closed-loop production optimisation. PhD thesis. University of Oklahoma, USA.

Fonseca, R.M., Stordal, A., Leeuwenburgh, O., Van den Hof, P.M.J. and Jansen, J.D, 2014: Robust ensemble-based multi-objective optimization. Proc. 14th European Conference on Mathematics in Oil Recovery (ECMOR XIV), Catania, Italy, 8-11 September.

Fonseca, R.M., Chen, B., Jansen, J.D. and Reynolds, A.C., 2017: A stochastic simplex approximate gradient (StoSAG) for optimisation under uncertainty. *International Journal for Numerical Methods in Engineering* 109 (13) 1756-1776. https://doi.org/10.1002/nme.5342

Hansen, N.: The CMA Evolution Strategy: A Tutorial, ArXiv e-prints, arXiv:1604.00772, 2016, pp.1-39.

Hansen, N.: A CMA-ES for Mixed-Integer Nonlinear Optimization, [Research Report] RR-7751, INRIA. 2011. <inria-00629689>.

Hansen, N., Niederberger, A., Guzzella, L., and Koumoutsakos, P.: A Method for Handling Uncertainty in Evolutionary Optimization with an Application to Feedback Control of Combustion. *IEEE Transactions on Evolutionary Computation*, Institute of Electrical and Electronics Engineers, 2009. <inria-00276216>.

Helgason, D., 2017: Algorithm for optimal well placement in geothermal systems based on TOUGH2 models. MSc Thesis. Reykjavik University, Iceland. http://hdl.handle.net/1946/26949

Kamel, A.H.: A technical review of radial jet drilling. *J. of Petroleum and Gas Eng.* **8**(8), (2017), 79-89. DOI: 10.5897/JPGE2017.0275

Kong, Y., Pang, Z., Shao, H. and Kolditz, O., 2017: Optimisation of well-doublet placement in geothermal reservoirs using numerical simulation and economic analysis. *Environmental Earth Sciences* 76 118 https://doi.org/10.1007/s12665-017-64044

Lensink, S. (ed.): Eindadvies basisbedragen SDE+ 2019: 2018 https://www.pbl.nl/publicaties/eind advies-basisbedragen-sde-2019.

Nair, R. Peters, E., Šliaupa, S., Valickas, R., Petrauskas, S.: A case study of radial jetting technology for enhancing geothermal energy systems at Klaipėda geothermal demonstration plant. Proceedings of the 42nd Workshop on Geothermal Reservoir Engineering, Stanford University, Stanford, California, 2017.

NTNU, FieldOpt Well Index Calculator, code link stored at https://libraries.io/github/ PetroleumCyberneticsGroup/FieldOpt-WellIndexCalculator. 2018.

Peters, E., Blöcher, G., Salimzadeh, S., Egberts, P.J.P., and Cacace, M.: Modelling of multi-lateral well geometries for geothermal applications. *Adv. Geosci*. **45**, (2018) 209-215. https://doi.org/10.5194/adgeo-45-209-2018.

Peters, E., Egberts, P., Chitu, A., Nair, R., Salimzadeh, S., Blöcher, G. and Cacace, M.: The Horizon 2020 SURE Project: Deliverable 7.4 - Upscaling of RJD for incorporation in reservoir simulators, Potsdam : GFZ German Research Centre for Geosciences (2019a) DOI: 10.2312/gfz.4.8.2019.003.

Peters, E., Blöcher, G., Nair, R., Geel, C.R. Salimzadeh, S.: The Horizon 2020 SURE Project: D7.5 – Comparison of RJD reservoir performance to conventional wells. Potsdam : GFZ German Research Centre for Geosciences (2019b)

Reinsch, T., Paap, B., Hahn, S., Wittig, V. and van den Berg, S. (2018) Insights Into the Radial Water Jet Drilling Technology - Application in a Quarry. Doi: 10.1016/j.jrmge.2018.02.001.

Troost, D. Optimization of Jetted Radial Wells. MSc Thesis, Delft University of Technology, 2019.

Yan, J., Cui, M., He, A., Jiang, W. and Liang, C. Study and Application of Hydraulic Jet Radial Drilling in Carbonate Reservoirs. *International Journal of Oil, Gas and Coal Engineering*. **6**(5), (2018), pp. 96-101. doi: 10.11648/j.ogce.20180605.13.